# Non-invasive Assessment of Packaged Cod Freeze-Thaw History by Hyperspectral Imaging

***Kathryn E. Washburn [a]*, Svein Kristian Stormo [a], Martin H. Skjelvareid [a] & Karsten Heia [a]***

* Corresponding author. E-mail: kathryn.washburn@nofima.no
[a] Department of seafood industry, Nofima AS, P.O. Box 6122, 9291 Tromsø, Norway

**Abstract**

*Freezing, storage and thawing all significantly affect the quality of seafood products. In this article, we explore the potential for estimating these parameters using online optical spectroscopic measurements. Fillets of cod were vacuum packed and underwent different programs of freezing, thawing and storage. Hyperspectral imaging of the fillets was performed at each program stage. Both single and double-frozen samples are studied. Different freezing and thawing methods are also investigated. Multivariate analysis of the hyperspectral data show that freezing history can clearly be determined on samples in the frozen state and to some degree on samples in the thawed state. Analysis of the data shows a less clear distinction between methods of thawing. Measurement on samples after a year of storage still showed the ability to classify samples based on their freezing history. These results show that hyperspectral technology can be used to evaluate the freeze-thaw history and potentially estimate quality of cod products in a manner that meets the speed and non-invasive requirements of an industrial setting.*

**Keywords:** hyperspectral imaging; fish, cod; storage; freezing; classification

## 1 INTRODUCTION

Freezing and thawing can lead to changes in seafood that affect both their sensory properties and market value. Because consumers believe fresh fish to be a superior product (Peavy et al. 1994), it commands a better market price than previously frozen fish. For frozen seafood, the freezing procedure may affect the product; both the rate of freezing (Pan and Yeh, 1993; Chen and Pan, 1997) and the freezing temperature (Mørkøre and Lilleholt, 2007) have been shown to influence changes that occur to fish during freezing, such as water loss, gaping, or toughness. Such changes can alter the perceived desirability and market price of the product. Refreezing of previously frozen samples has been shown to negatively affect sensory properties of fish such as toughness, dryness, fibrousness and fishy smell (Kent et al. 2004). Fish that have been twice-frozen deteriorate more rapidly in sensory quality under long term storage compared to fish that have been frozen only once (MacCallum et al. 1966; Desrosier and Tressler, 1977). In particular, if the initial freezing of the twice-frozen samples was performed using poor freezing conditions, this led to a significantly shorter shelf life of the fish

(Desrosier and Tressler, 1977). All these reasons highlight the importance for companies to have control over the freeze-thaw history of their seafood products.

Ensuring the product delivered to the consumer is the product promised is vital for companies to protect brand reputation. A challenge to the fish processing industry is that a delivery may not consist of fish that have experienced identical handling. A delivery may be comprised of catches from several different vessels, each with different equipment capabilities and handling procedures. Furthermore, previously frozen fish may be purposely mixed in with fresh fish due to the higher market price. These issues make detection of fish of unacceptable quality by spot checks challenging. Therefore, there is a demand for evaluation methods rapid enough to be performed on every fish. Such measurements can potentially be used to detect fraud (e.g. frozen-thawed fish sold as fresh) and measuring if a product has been handled according to the standard set by the buyer. Investigation of double freezing is especially relevant for products based on fish frozen at sea. Here, the fish is thawed before processing (e.g. filleting) and subsequently frozen again as a finished product and proper freezing and thawing parameters are vital if high quality is to be maintained. In this work, we investigate if measurements can be made to determine the full freezing history of double-frozen products.

Previous research has investigated a variety of techniques to distinguish between fresh, once-frozen and twice-frozen seafood. Differential scanning calorimetry found a difference in the denaturation temperatures between fresh, once-frozen and twice-frozen gilthead seabream (Matos et al. 2011). Time domain reflectometry to estimate dielectric constants of minced cod was able to differentiate between once-frozen and twice-frozen samples with good accuracy (Kent et al. 2004). Similarly, dielectric measurements in the frequency domain showed the ability to distinguish between fresh, once-frozen and twice-frozen sea bass (Vidacek et al., 2008). Raman spectroscopy was able to reliably identify fresh, once-frozen, and twice-frozen cod by measuring on fat extracted from thawed samples. (H.M. Velioğlu et al., 2015). While all these techniques have proven successful in a lab environment, they take from minutes to hours to perform and frequently require alteration of the sample (e.g., mincing, extraction, etc.). Therefore, the measurement time and extensive sample handling they require make them not suitable for high-throughput industrial screening, where approximately one fillet per second needs to be scanned.

In this article, hyperspectral imaging was assessed as a method to evaluate the freeze-thaw history of seafood. This technology has been applied previously to perform many different types of quality control in a wide range of foods (Sun 2010, Siche 2016). Hyperspectral measurement is appealing compared to other forms of spectroscopy, such as Raman or nuclear magnetic resonance, because it is both non-invasive and rapid. Optical spectroscopy is a well-established method for material characterization. When light interacts with a material, some wavelengths will be absorbed while others will pass through the material. The amount of light absorbed by or transmitted through a sample depends on both its structure and its composition. Therefore, by analyzing how a sample absorbs light at different wavelengths, information can be gained on its properties. Hyperspectral imaging is a form of spatially resolved optical spectroscopy. In traditional imaging, each pixel has an intensity associated with a single wavelength for gray scale images or intensities at three different wavelengths for color images. In hyperspectral imaging, every pixel is associated with a plurality of wavelengths that can be used to evaluate the structure and composition of that location in the sample.

The hyperspectral images analyzed in the present study were acquired using the interactance acquisition mode (Schaare and Fraser, 2000). Here, light travels through the sample and the reemitted light is measured to determine which wavelengths have been absorbed. Interactance spectroscopy differs from transmission spectroscopy in that it measures light that has traveled back to the illuminated surface as opposed to light that has passed through the sample. The method is useful for

samples where complete transmission is not possible, for example if the sample is very thick or where opaque constituents are present. Another practical advantage is that one-sided measurement enables imaging on conveyor belts where only one side of the sample is accessible. Interactance is also useful when the sample thickness is variable and would lead to an inconsistent transmission path length.

This work builds upon previous research where it was observed that fresh and previously frozen samples could be clearly distinguished using hyperspectral measurements on thawed samples (Sivertsen et al. 2011, Zhu et al. 2013). There are several aims to this study. First, the scope of investigation is expanded to evaluate whether these techniques can distinguish between fresh, once freeze-thawed and twice freeze-thawed products. Secondly, we evaluate if the freeze-thaw history can be estimated based on measurements on samples in the frozen state. Furthermore, this study also seeks to determine whether hyperspectral measurements can identify the freezing and thawing procedures the samples had experienced.

# 2 MATERIALS AND METHODS

## 2.1 HYPERSPECTRAL IMAGING EQUIPMENT

Figure 1 shows a diagram of the hyperspectral imaging setup.

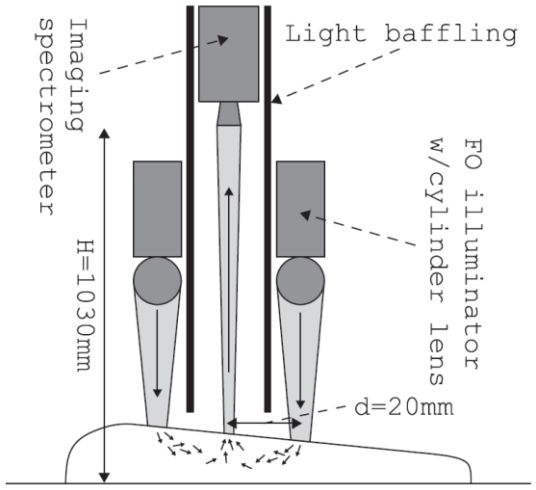


*Figure 1: Diagram of the hyperspectral imaging setup. Note that to save space, the vertical scale of the figure has been compressed*

The illumination source was a pair of fiber optic line lights, each 200 mm wide and powered by three 150 W halogen lamps. To maximize the amount of NIR light directed into the fiber optic system, lamps with a special aluminum coating were used (International Light Technologies, lamp model L1090). Cylindrical lenses mounted in front of the line lights focused the light into two 10 mm thick parallel lines, 40 mm apart. The camera line of view was placed between the light lines, resulting in a 20 mm distance to each of the lines, as shown in Fig. 1. Previous work has shown that dual illumination of the sample improves signal to noise compared to a single illumination source, as well as resolves the problem of being unable to obtain a signal at the edges of the sample (Sivertsen et al. 2009; Wold et al. 2006). Two aluminium light baffles painted black were used to block light which would otherwise illuminate the sample directly in the camera line of view. The fiber optic line lights and detector were mounted at heights of 150mm and 1030 mm respectively above the conveyor belt. The detector used

was a VNIR-1024 from Norsk Elektro Optikk (Skedsmokorset, Norway). The hyperspectral camera operates in the VIS-NIR range from 430 to 1000 nm.

The hyperspectral camera field of view is 0.56 mm x 300 mm. Each pixel is 0.28 mm x 0.56mm in size and light from that area is measured in the 430-1000 nm spectral region with approximately a 5.4 nm resolution. The region of detection is centered parallel between the two illumination lines. Imaging of the samples was performed on a conveyor belt traveling at 40 cm/s, a rate that meets the industrial production requirement of approximately one fillet per second. Each sample was scanned line by line at 400 frames per second as it moved through the hyperspectral camera field of view. The data is stored as a hyperspectral image $R_i(\lambda, x, y)$ consisting of successive frames $F(\lambda, x)$. Calibration of the system was performed using a 300 mm square Teflon target of 25mm thickness. The average reference frame $R_a(\lambda, x)$ was calculated from one hundred successive frames of the Teflon target. The absorption of the interactance images are calculated as $I(\lambda, x, y) = -\ln(R_i(\lambda, x, y)/R_a(\lambda, x))$ where $R_i(\lambda, x, y)$ is the hyperspectral image of the packaged cod loin.

## 2.2 FISH SAMPLES

Atlantic cod for the study were procured by capture based aquaculture. Here, wild cod are captured with seine nets in the spring and then held in sea cages for later slaughter. This both minimizes stress on the fish and allows for better control of the slaughter process, enabling the supply of high quality fish in the months traditionally out of season by conventional fishing. The cod were stored and fed at the Tromsø Aquaculture Research Station, Norway and were killed by a blow to the head and immediately gutted. They were bled for 30 minutes, iced and transported to Nofima, where they were kept on ice for two days prior to filleting. These procedures helped ensure that uniformly high quality fish were used in the study to minimize potential confounding effects resulting from defects (e.g. inadequate bleeding) caused by poor sample handling. The back loin was used for the experiments. Each loin was cut in 2 or 3 pieces (179 ± 32 g), depending on the size of the fish. The loin-pieces were then vacuum-packed (pressure 10 millibar) in plastic pouches (20 µm polyamide inside layer and 70 µm polyethylene outside layer) and kept on ice until the first imaging and subsequent freezing and frozen storage.

The two hundred vacuum packed loin pieces of cod were divided into forty groups (n=5). The groups each underwent a different program of freezing, thawing and measurement; the samples were kept vacuum packed for the entire program to minimize the influence of additional factors besides freezing, thawing and frozen storage. Two modes of sample freezing were used: blast freezing at -40° C (fast) and freezing in still air at -20°C (slow). Two modes of sample thawing were used: in 4° C circulating water (fast) and at 4°C by gently circulating air in a climate controlled cabinet (slow). The different freeze-thaw procedures and measurement stages are shown in Figure 2. Every sample in a group underwent the same sequence of freezing, thawing and measurement as the others in the group. All frozen samples were brought to equilibrium at -20° C before hyperspectral measurement to avoid temperature effects producing a bias in the measured spectra.

In stage A, samples were vacuum-packed and hyperspectral measurements were performed on all samples. In stage B, the samples were frozen using one of the two different freezing protocols. After freezing, samples were all kept at -20 °C for two days and then hyperspectral measurements were repeated on all the samples in the frozen state. Some samples were placed in long term storage at -20°C (Stage F) and the remaining samples moved onto Stage C. Here, they were thawed using the two different thawing protocols and hyperspectral measurement performed. In stage D, the remaining samples were refrozen. Some samples maintained the same freezing protocol for the second freezing as the first freezing. Others changed freezing protocols between the two freezings -- i.e. samples first

frozen using the fast protocol were refrozen using the slow freezing protocol and vice versa. Again, the samples were kept at -20°C for two days and then the twice-frozen samples underwent hyperspectral measurement in the frozen state. Again, a set of samples were removed for long term storage. The rest of the samples moved onto Stage E, where they were thawed for hyperspectral measurement. In Stage E, there existed a sample group that covered every permutation of fast and slow freezing and fast and slow thawing for twice-frozen samples. For Stage F, hyperspectral measurements were made on the samples in the frozen state at the end of storage. The long term storage samples were stored in a freezer at -20 °C for 12 months. Finally in Stage G, the samples were thawed and the final hyperspectral measurements were performed. As with Stages C and E, in Stage G a complete set of samples existed that covered all the possible permutations of freezing and thawing protocols for both once and twice-frozen samples.

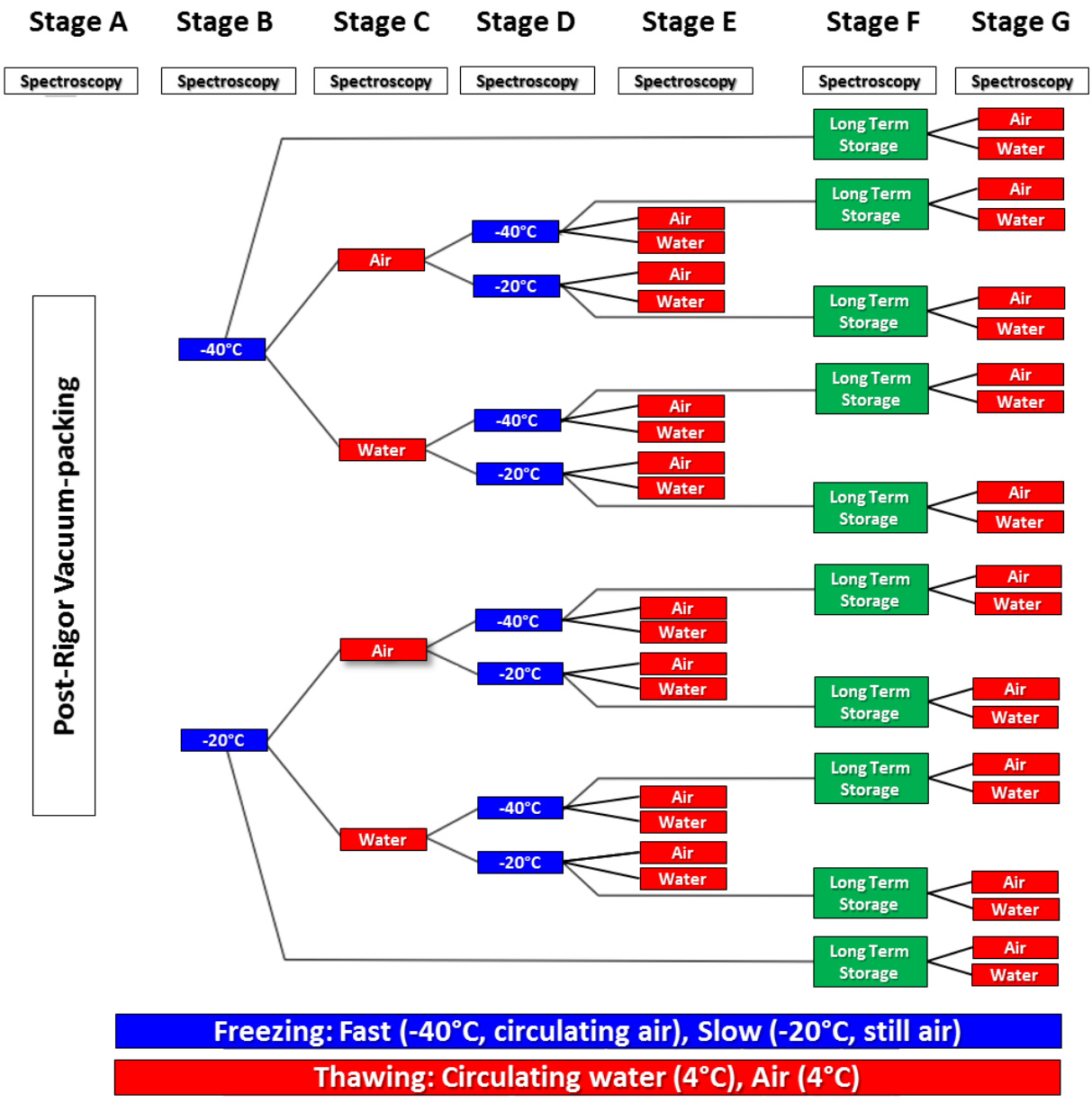


*Figure 2: Program of Analysis. Stage A - vacuuming packing and measurement on the samples in the fresh state. Stage B – first freezing of samples and hyperspectral measurement on the samples in the frozen state. Stage C – first thawing of samples and hyperspectral measurements of the samples in the thawed state. Stage D – second freezing of samples and hyperspectral measurement on the samples in the frozen state. Stage E – second thawing of samples and hyperspectral measurements of*

*the samples in the thawed state. Stage F – hyperspectral measurement of samples in the frozen state that have undergone long term storage frozen Stage G – hyperspectral measurement of samples in the thawed state that have undergone long term frozen storage.*

## 2.3 Data Analysis

Extraction of hyperspectral data for analysis was performed using IDL (Exelis Visual Information Solutions, Bracknell, United Kingdom). Regions of interest were manually selected for each sample. Regions were selected in the center of the sample, avoiding areas with sample defects (e.g. blood clots) or image aberrations (e.g. reflections, distortions, etc.). All spectra from the region were exported from IDL in the raw form and further analysis was performed using the R programming language (Free Software Foundation Inc., Boston, MA). Spectra were area normalized, averaged to a single spectrum for each sample and the first derivative taken. Taking the first derivative makes subsequent analyses more sensitive to small differences between the spectra as well as to correct for baseline effects. No smoothing was applied. Principal component analysis (PCA) (Wold et al. 1987) was then performed using three different approaches: examining the entire spectrum, examining only the region of 450-600nm, which is associated with blood in the fish (Olsen and Elvevoll, 2011), and examining the region of 900-990 nm, which is associated with water (Hale and Query, 1973; Pope and Fry, 1997). The spectra were analysed using the different region selections in order to evaluate whether a particular sample constituent was predominant in the ability to assess a samples freeze-thaw history. As using extraneous information in multivariate analysis typically leads to worse predictions (Anderssen et al., 2006), it is considered good practice to limit analysis to wavelengths known to be associated with the effect to be measured. For example, previous research found that limiting analysis of VIS-NIR measurements on cod to the visual region (450-700 nm) improved prediction results for refrigerated storage time (Nilsen et al. 2002) and differentiation between fresh and once-frozen samples in the thawed state ( Sivertsen et al. 2011).

The spectra were scaled and centered during principal component analysis. After principal component analysis, classification was performed using k-nearest neighbors classification (Cover and Hart, 1967). The k-nearest neighbors (kNN) algorithm is a form of supervised learning, where a set of samples with known classifications are used to predict the classification of new samples. New samples are predicted by assigning a classification based on the classifications of the nearest samples to the new sample in the variable space. K-nearest neighbors cross-validation was performed here on the full set of principal components using 3 nearest neighbors by the “Leave One Out” method; one sample was left out of the data set and the remaining samples were used to predict its classification. This was repeated for all samples.

# 3 Results

## 3.1 Differentiation of freezing method

Figure 3 shows the result of principal component analysis on the once-frozen samples measured in the frozen state. Table 1 contains information on k-nearest neighbors accuracies. Analysis on the

entire spectrum shows good separation between the two freezing methods. For analysis performed using the 450-600 nm region, while clustering is less prominent in the first principal component, the two groups can be distinguished visually when examined using the second and third principal components. Analysis using the water region of the spectra showed the best separation; the two freezing methods show clear separation in the first principal component. K-nearest neighbors analysis showed the two groups could be classified with excellent accuracy. The kNN prediction for the entire spectrum identified both freezing protocols with 100% accuracy. Using the 450-600 nm region, the -40°C samples were predicted with 98% accuracy and the -20°C samples with 99% accuracy. For the analysis using only the water region of the spectrum, again both freezing protocols could be predicted with 100% accuracy.

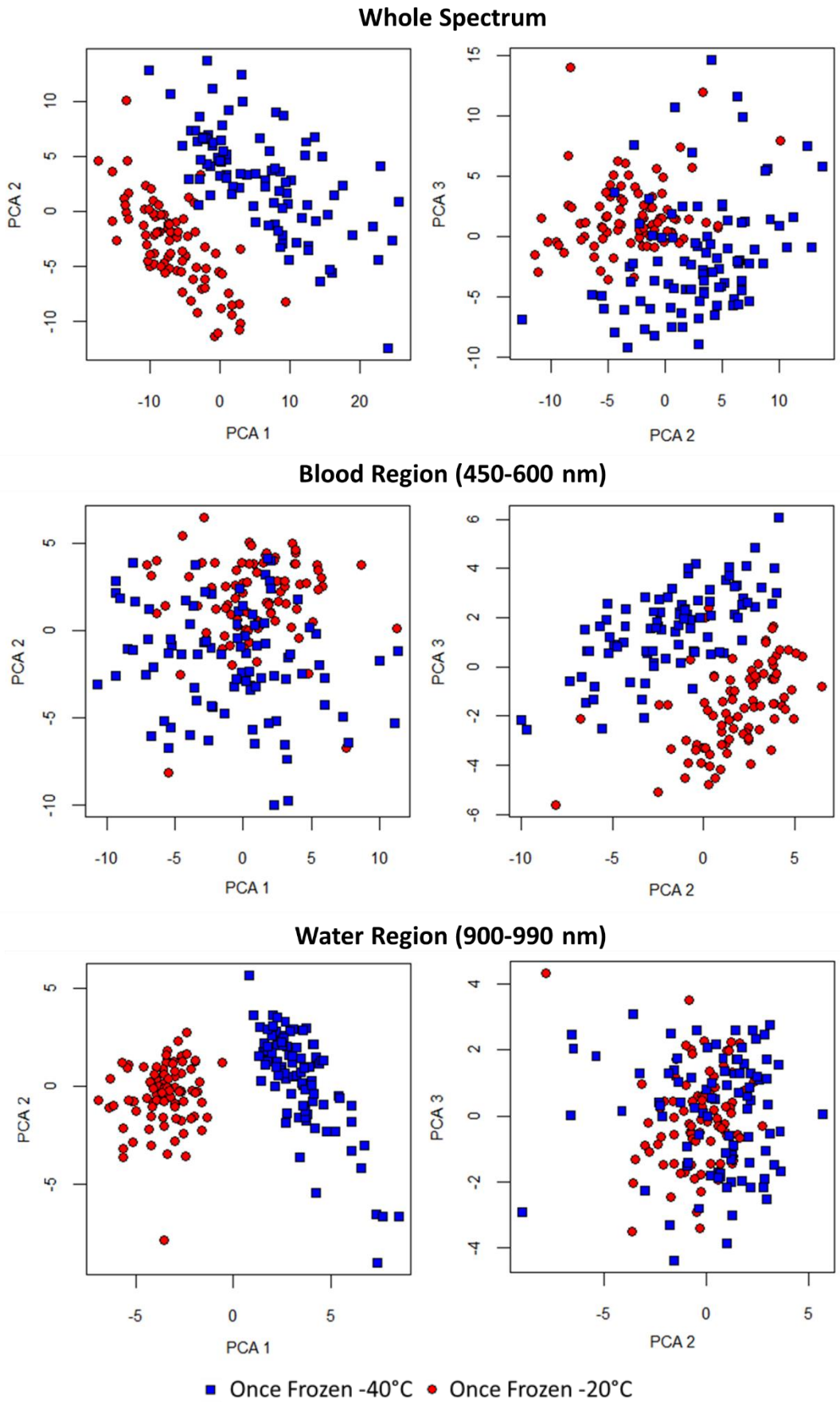


 *Figure 3 Principal component analysis on once-frozen samples measured in the frozen state*

*Table 1: K-nearest neighbors classification accuracies of freezing protocol for once-frozen samples in the frozen state*

| Sample Type | Full Spectrum | 450-600 nm | 900-990 nm |
|---|---|---|---|
| Frozen -40°C | 100% | 98% | 100% |
| Frozen -20°C | 100% | 99% | 100% |

## 3.2 Influence of Freezing and Thawing Method in Once-Thawed Samples

Figure 4 shows the PCA scores plot of the spectra on the once-frozen samples in the thawed state using the entire spectrum for analysis. Table 2 contains the k-nearest neighbor classification accuracy for the thawed samples by freezing protocol, by thawing protocol, and by both freezing and thawing protocol. Regardless of the region of the spectrum used for analysis, there appeared to be no visually consistent grouping of the samples by either freezing method or thawing method used. K-nearest neighbor classification of the samples by freezing protocol showed poor classification, ranging from 38% to 58% regardless of which region of the spectrum had been used for analysis. K-nearest neighbor classification by thawing method performed marginally better, with prediction accuracies ranging from 45% to 64%. Classification by both freezing protocol and thawing method simultaneously performed very poorly, with accuracies ranging from 9% to 53%.

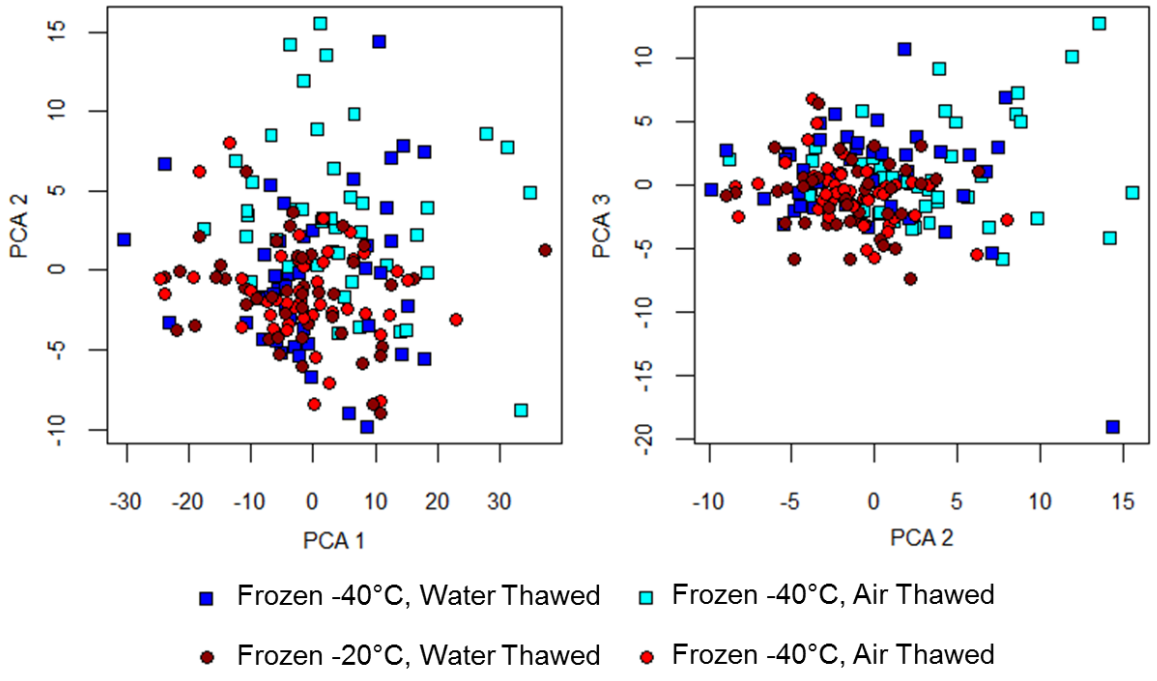


*Figure 4 Principal component analysis on once-frozen samples measured in the thawed state.*

*Table 2: K-nearest neighbors classification accuracies for freezing protocol for once-thawed samples measured in the thawed state, for thawing protocols of once-thawed samples measured in the thawed state, and for both freezing and thawing protocol for once-thawed samples measured in the thawed state*

| Sample Type | Full Spectrum | 450-600 nm | 900-990 nm |
|---|---|---|---|
| Frozen -40°C | 58% | 56% | 53% |
| Frozen -20°C | 38% | 38% | 47% |
| Thawed Air | 60% | 64% | 57% |
| Thawed Water | 45% | 51% | 50% |
| Frozen -40°C, Thawed Air | 51% | 53% | 42% |
| Frozen -40°C, Thawed Water | 20% | 20% | 26% |
| Frozen -20°C, Thawed Air | 22% | 22% | 9% |
| Frozen -20°C, Thawed Water | 31% | 27% | 36% |

## 3.3 Differentiation of Once and Twice-frozen Samples

Figure 5 shows the PCA of the once and twice-frozen samples in the frozen state for the entire spectrum. Table 3 shows the k-nearest neighbor classification accuracies for once and twice-frozen samples, for freezing protocol in once and twice-frozen samples evaluating only the last freezing for the twice-frozen samples, and for freezing protocol in once and twice-frozen samples evaluating both freezings for the twice-frozen samples. The samples could be classified into once-frozen and twice-frozen with good accuracy, with success rates ranging from 97%-100%. Similarly, classification of the samples by freezing protocol produced very good results. K-nearest neighbor prediction using the entire spectrum had almost perfect classification. Analysis using the blood region of the spectrum was still very good, but had slightly more misclassified samples. Analysis using the water region alone accurately identified the freezing protocol for the once-frozen samples, but had a few misclassifications in the twice-frozen samples.

For all approaches, the second freezing in the twice-frozen samples appeared to be the dominant effect. Reliable separation of twice-frozen samples by their initial freezing protocols did not appear to be possible. Accuracy of prediction for first freezing protocol on the twice-frozen samples ranged from 40% to 67%. For context, completely random prediction of the four different possible freezing histories would produce results with roughly 25% accuracy.

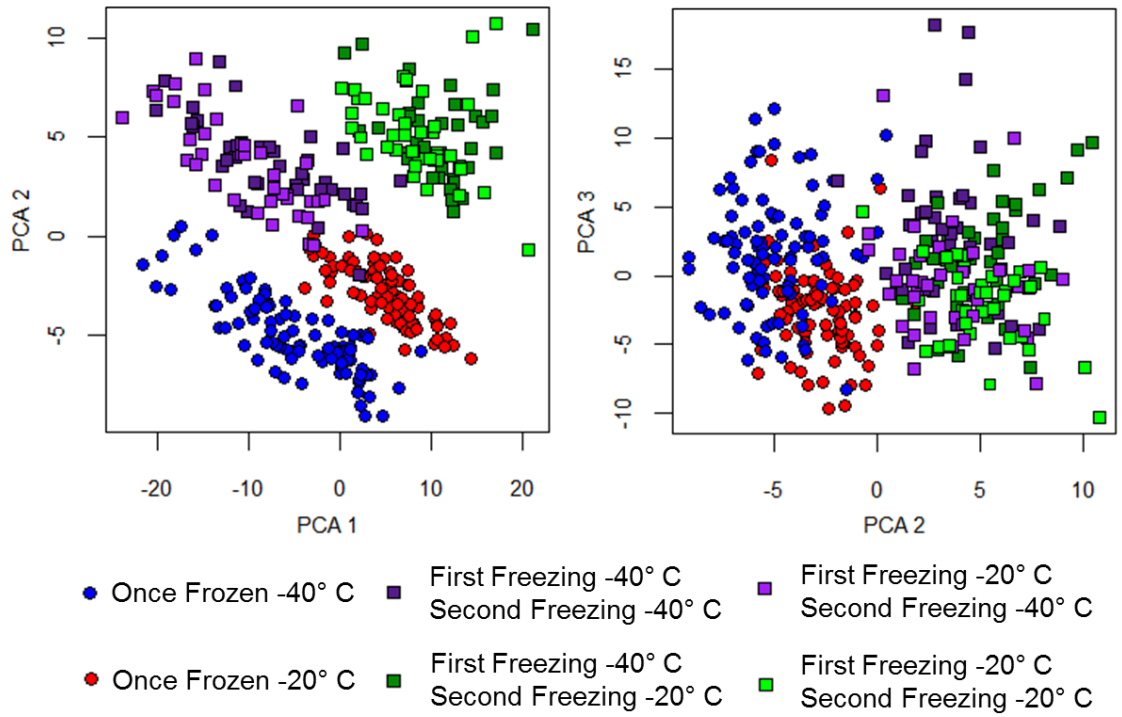


*Figure 5: Principal component analysis for once and twice-frozen samples measured in the frozen state*

*Table 3: K-nearest neighbors classification accuracies for once and twice-frozen samples measured in the frozen state, for freezing protocol in once and twice-frozen samples measured in the frozen state, and for freezing protocol in once and twice-frozen samples. For twice-frozen samples, both first and second freezing protocol were evaluated for classification*

| Sample Type | Full Spectrum | 450-600 nm | 900-990 nm |
|---|---|---|---|
| Once-frozen | 100% | 99% | 100% |
| Twice-frozen | 98% | 97% | 95% |
| Once-frozen -40°C | 100% | 99% | 100% |
| Once-frozen -20°C | 100% | 97% | 100% |
| Twice-frozen, last freezing -40°C | 95% | 86% | 92% |
| Twice-frozen, last freezing -20°C | 100% | 95% | 97% |
| Once-frozen -40°C | 100% | 99% | 100% |
| Once-frozen -20°C | 100% | 97% | 100% |
| Twice-frozen -40°C, -40°C | 50% | 40% | 63% |
| Twice-frozen -40°C, -20°C | 54% | 56% | 59% |
| Twice-frozen -20°C, -40°C | 60% | 50% | 53% |
| Twice-frozen -20°C, -20°C | 67% | 59% | 62% |

## 3.4 Differentiation of Fresh, Once-thawed and Twice-thawed Samples

Figure 6 shows the analysis of fresh, once-thawed and twice-thawed samples. Table 4 contains the k-nearest neighbor classification accuracies for fresh, once-thawed and twice-thawed samples. These groups contain all possible permutations of fast and slow thawing parameters for the once and twice thawed samples. As was seen previously (Sivertsen et al., 2011) the fresh and thawed samples can be readily distinguished from one another. In all classifications, fresh samples could be reliably distinguished from thawed samples. Analysis of the entire spectrum produced the best classification of the thawed samples, with 98% and 93% correct classification for the once and twice-thawed

samples. Analysis using the water region produced the worst classification, with 91% and 75% accuracy for once and twice-thawed samples respectively.

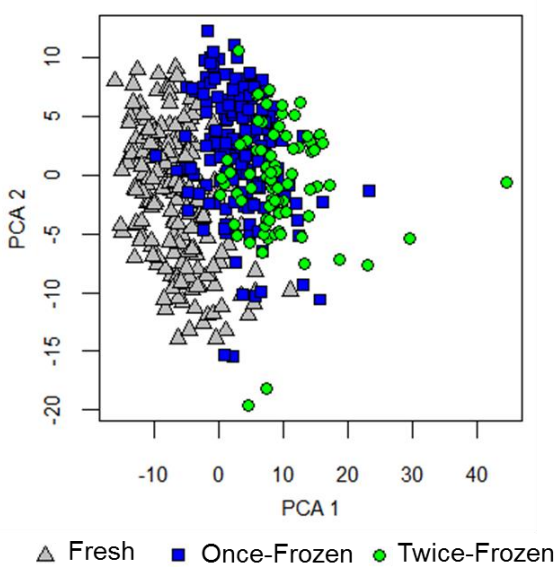


*Figure 6 Principal component analysis for fresh, once-frozen and twice-frozen samples in the thawed state*

*Table 4: K-nearest neighbors classification accuracies for fresh, once-thawed and twice-thawed samples measured in the thawed state*

| Sample Type | Full Spectrum | 450-600 nm | 900-990 nm |
|---|---|---|---|
| Fresh | 100% | 100% | 99.5% |
| Once-thawed | 98% | 96% | 91% |
| Twice-thawed | 93% | 81% | 75% |

## 3.5 Effects After Long Term Frozen Storage

For the samples that underwent long term frozen storage, due to changes in the illumination source between the initial measurements and the measurements made after the storage period, the data from the two cannot be directly compared. Therefore, measurements of the long-term storage samples were only compared to one another, and not compared to measurements performed before the long-term frozen storage. Figure 7 shows the PCA analysis for the stored samples measured in the frozen state using the entire spectrum; Table 5 contains the k-nearest neighbors prediction accuracies for the stored samples in the frozen state by number of freezing cycles and by freezing protocol. Figure 8 shows the PCA analysis of thawing history for the stored samples measured in the thawed state, Table 6 contains the k-nearest neighbor prediction accuracies for the stored samples in the thawed state by number of freeze-thaw cycles and by freezing parameters.

Compared to the results on samples measured before frozen storage, there is a less clear distinction between the different freezing protocols, but clustering can still be observed in frozen samples that have undergone long term frozen storage. Once and twice-frozen samples can be differentiated between with 85-95% success rate when either the entire spectrum or the 450-600 nm region is used. Analysis on the water region alone produced significantly worse classification for the once-frozen

samples, but this may be an artifact of the small sample set. The last freezing protocol could also be identified using the entire spectrum with good results on the frozen samples after long term frozen storage. Analysis using the blood region or the water region alone produced significantly worse classification results for the freezing protocol, particularly in the once-frozen samples. As with the samples that had not undergone long term frozen storage, identification of the first freezing protocol for twice-frozen samples was not possible.

Analysis of the thawed samples showed the ability to predict the freezing history of the samples using the entire spectrum. Classification of once-thawed samples using the blood or water regions alone performed poorly. The classification of the twice-thawed samples generally performed well, but the classification of the once-thawed samples performed significantly worse. This may simply be statistical noise due to the low number of once-thawed samples; there were eighty twice-frozen samples but only twenty once-frozen samples that were placed in long term storage. The technique also produced poor classification of samples by freezing protocol. Given the inability to determine freezing protocol on the thawed samples before storage, the inability to do so after long term frozen storage is not surprising.

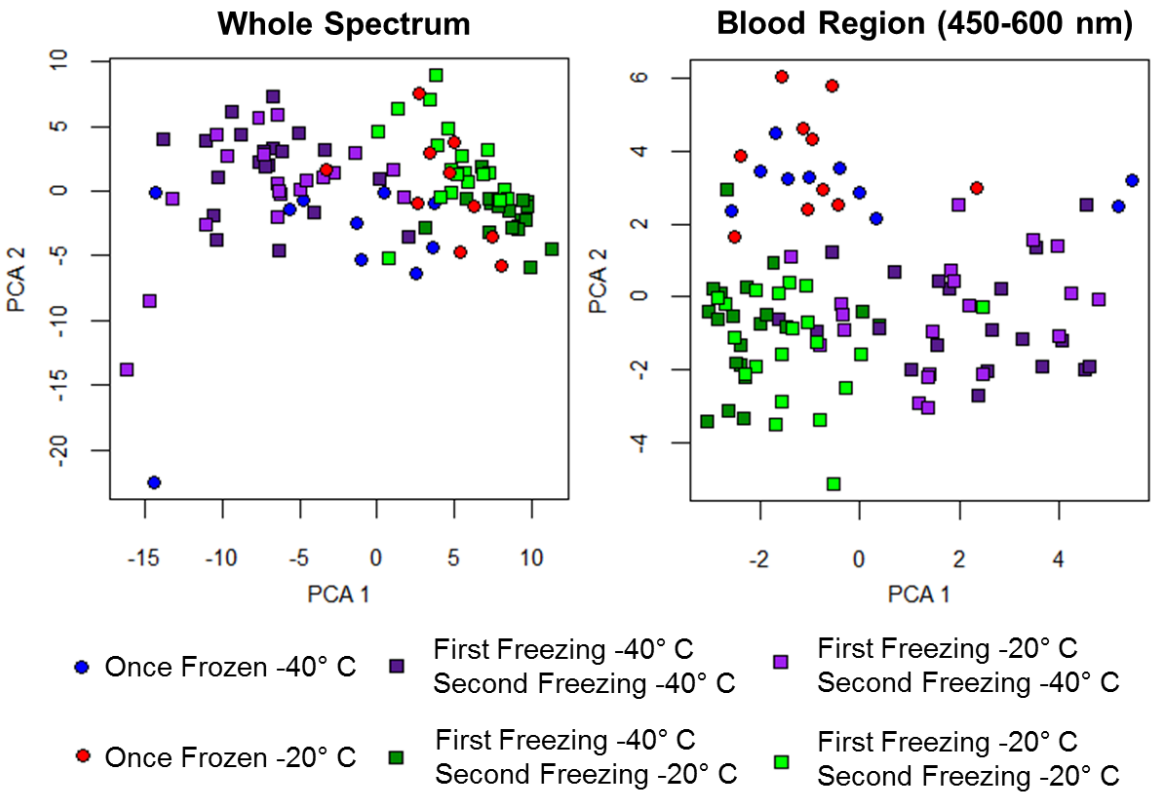


*Figure 7 Principal component analysis using the entire spectrum of freezing history for samples after long term storage measured in the frozen state.*

*Table 5: K-nearest neighbors classification accuracies for the number of freezings and for freezing protocol for once and twice-frozen samples after long term frozen storage measured in the frozen state. For twice-frozen samples, only the freezing protocol for the second freezing was evaluated for classification*

| Sample Type | Full Spectrum | 450-600 nm | 900-990 nm |
|---|---|---|---|
| Once-frozen | 80% | 85% | 15% |
| Twice-frozen | 96% | 95% | 80% |
| Once-frozen -40°C | 70% | 50% | 10% |
| Once-frozen -20°C | 90% | 80% | 10% |
| Twice-frozen, last freezing -40°C | 85% | 73% | 68% |
| Twice-frozen, last freezing -20°C | 98% | 90% | 85% |

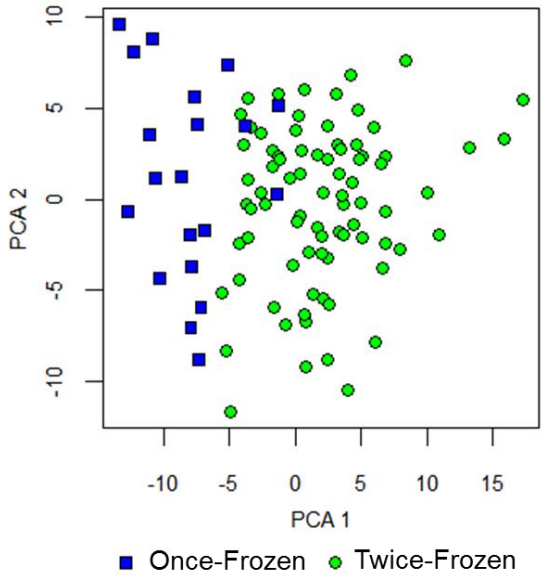


*Figure 8: Principal component analysis using the entire spectrum for the freezing history of samples after long term frozen storage measured in the thawed state.*

*Table 6: K-nearest neighbors classification accuracies for the number of thawings and freezing protocol for once and twice-frozen samples after long term frozen storage measured in the thawed state. For twice-frozen samples, only the freezing protocol for the second freezing was evaluated for classification*

| Sample Type | Full Spectrum | 450-600 nm | 900-990 nm |
|---|---|---|---|
| Once-thawed | 75% | 50% | 45% |
| Twice-thawed | 93% | 96% | 86% |
| Once-frozen -40°C | 40% | 30% | 50% |
| Once-frozen -20°C | 50% | 30% | 10% |
| Twice-frozen, last freezing -40°C | 45% | 50% | 50% |
| Twice-frozen, last freezing -20°C | 40% | 43% | 43% |

# 4 DISCUSSION

The results show that hyperspectral imaging can be used to reliably predict some aspects of the freeze-thaw history of a packaged fish sample. An unexpected result was the ability to much better identify the freeze-thaw history of the samples in the frozen state than in the thawed state. Analysis of hyperspectral images can accurately predict, in the frozen state, whether a sample is once or twice-

frozen. Reliable discrimination of whether the frozen samples were frozen quickly at -40°C or slowly at -20°C is also possible, but only for the last freezing if the sample is twice-frozen. For samples in the non-frozen state, it appears possible to determine whether the samples are fresh, once-thawed or twice-thawed. These capabilities appear to hold even after twelve months of storage at -20°C. However, estimation of the reliability of prediction for the samples that underwent long term storage was hampered by the small sample set; a larger study will need to be performed to better understand the accuracy and limits of the technique on samples that have undergone long term frozen storage.

Given the approach used here, it does not appear possible to determine the first freezing protocol for twice-frozen samples. Similarly, information regarding the freezing protocol used appeared to be lost during the thawing process, as analysis on data from the thawed samples could not accurately discriminate those that had been frozen quickly at -40°C from those that had been frozen slowly at -20°C. Discrimination of the thawing protocol used also did not appear to be possible.

For this study, while separating the spectra into different regions appeared useful for visual analysis of the sample clustering and to help understand the physical processes behind the analysis, using the entire spectrum for classification appears to be the superior approach. Curiously, analysis performed using both the blood and water regions of the spectrum simultaneously typically performed marginally worse than the classifications performed on the regions individually. Inspection of the full-spectrum loading values for the first principal component for the frozen samples, shown in Figure 9a, shows a peak at the 800-840 nm region that is not known to be associated with any particular sample constituent. In the loading values for the thawed samples, shown in Figure 9b, the peak is shifted to the 750-800 nm region. Previous researchers have seen the 760 nm OH stretch in water shifts towards 800 nm with increased ice fraction (Ottestad et al. 2009), which is what we believe is occurring here. We expect this behavior is the reason the full spectrum analyses generally were superior to the blood or water region analyses.

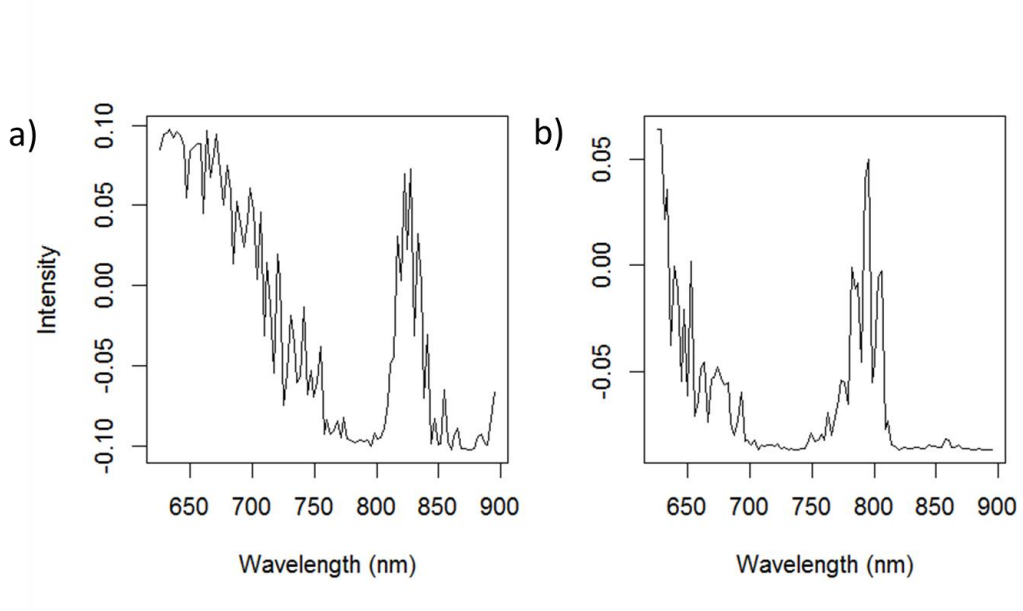


*Figure 9: PCA 1 Loadings for the entire spectrum analysis for a) Once-frozen samples in the frozen state b) Once-frozen samples in the thawed state*

Based on what we are and are not able to predict, we believe that the structure and quantity of ice in the frozen samples plays an important role in the ability to determine the last freezing protocol used.

Despite the sample being frozen, some water in the tissue may remain in liquid form due to freezing point depression. For cod, it has been found that the quantity of unfrozen water decreases down to -33°C, where it remains stable at approximately 5% (Tolestorebrov et al. 2014). This super-cooled water, once-frozen, will remain frozen even when heated back to -20 °C, though structural changes to the ice may occur (Syamaladevi et al. 2012). Previous research on frozen salmon has shown that different freezing temperatures will also result in different size and shapes of ice crystals in the fish flesh (Syamaladevi et al. 2012). Scattering of light as it travels through the sample is affected by crystalline structure, which would then be detectable by the hyperspectral measurement. This would also explain why analysis on the thawed samples was unable to classify samples by their freezing temperature history.

Even though classification using the spectral range associated with blood was less accurate than using the full spectrum or the water region of the spectrum, good classification of freezing protocol was still possible for the frozen samples. If this was due to the different freezing processes causing chemical changes to the blood, such as oxidation, these effects should still be detectable in the thawed state, which they were not. Therefore, it is believed the spectral changes associated with freezing protocol in the blood region mainly arise from light scattering effects, which by nature span the whole spectral range measured (Jacques 2013). Much of this likely is associated with the ice formation. There may also be an additional scattering effect that arises from the blood itself due to the hindered molecular rotation during freezing. Future work is planned to test these theories and better understand the changes that occur to the tissue during the freezing processes.

Averaged spectra for the fresh, once thawed and twice thawed samples are shown in Figure 10. In Sivertsen et al. (2011), the results indicated that changes in the oxidation state of blood allowed the discrimination between fresh and once-frozen samples. While the thawed spectra in this study also show indications of oxidation, the changes are less than might be expected given the duration of the program. This is attributed to the vacuum packing of the samples, such that the available oxygen is minimal. In this study, the ability to discriminate between the fresh, once thawed and twice thawed samples appears to depend on increased light scattering with each freeze-thaw cycle. This effect is prominently observed by the increased wavelength dependent baseline shift in the spectra in the 450 to 600 nm region with each freeze-thaw cycle. The increased light scattering is attributed to denaturation of proteins during freezing and thawing (Love 1962).

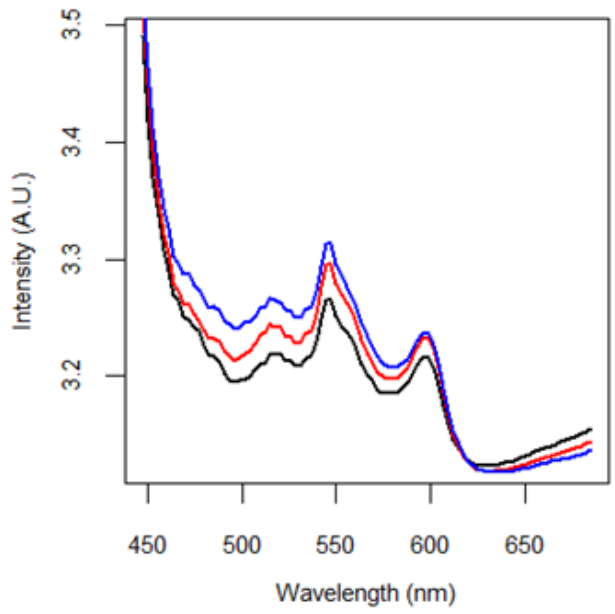

*Figure 10: Averaged absorbance spectra for fresh (black), once thawed (red) and twice thawed (blue) samples*

Examination of the plot of the first and second components of the once and twice-frozen samples (Fig. 5) shows an interesting trend. All the once-frozen -40°C samples cluster in the lower left quadrant. Moving up and to the right, we see the clusters of the once-frozen at -20°C and twice-frozen with the second freezing at -40°C. Finally, the twice-frozen samples with the second freezing at -20°C cluster in the upper right quadrant. We speculate that movement along this axis from lower left to upper right quadrant may be related to fish quality attributes. Samples frozen at a lower temperature have been shown to have characteristics associated with higher quality (e.g. less water loss, gaping, etc.). Similarly, twice-frozen samples have been shown by previous researchers (Kent et al. 2004) to have more undesirable characteristics such as toughness, dryness and fishy smell. How characteristics of samples once-frozen at -20°C compare to twice-frozen at -40°C is unknown; to the authors' knowledge, no studies in the literature exist that compare these situations. Future work is planned to compare sample location on this axis to other quantifiable properties that previous research (Bonilla et al. 2007, Warm et al. 1998) has shown to be associated with perceived high and low quality in cod such as appearance, texture, odor and flavor.

While the results here are promising, there are important differences in the study compared to real world conditions. It is unrealistic that a sample's entire freeze-thaw history would occur in the vacuum packed, filleted state. For twice-frozen products, the first freezing would occur at sea with the fish being headed, gutted and frozen whole. The fish would then be thawed ashore for filleting, and then refrozen. Also, measurements were performed on a section of cod loin in samples that had been handled to produce high quality fillets. How robust the results are in other sections of fish, species of fish or in fish that have had less than ideal handling are unknown. Therefore, generalizations of results of this study to other situations need to be treated with caution.

With these considerations in mind, there exist potential applications of the results at the industrial scale. There are multiple stages at which freezing procedure control could be relevant. For the fish processing industry, the speed and non-invasive nature of hyperspectral imaging make it an excellent technology for online quality control when buying deliveries of fish; samples can easily be measured at a rate compatible with online sorting equipment. While region selection was performed manually here, this type of task could be easily automated using standard image analysis methods. This means that fish could be automatically sorted by different handling protocols as they can be currently sorted by size today. A delivery could be sorted into different batches based on freezing protocol used or number of freezings undergone. By sorting the fish by handling procedure, and by proxy the perceived quality, this would enable the maximum price to be obtained for a delivery as quality is currently assigned to a whole batch by the lowest quality specimens. For buyers of finished frozen seafood products, such as a supermarket chain, the technology would enable them to confirm the product has been handled as stated and avoid overpaying for lower quality product. Similarly, there may exist situations where the end buyer also wishes to evaluate the freeze-thaw history of seafood products, for example to confirm that the products have not been allowed to thaw during transport and then refrozen later.

# 5 CONCLUSIONS

We demonstrate here that hyperspectral imaging has the potential for use as an online method for evaluation of sample freeze-thaw history. It is possible to differentiate between the freezing protocols

on packaged samples in the frozen state. In the thawed state, differentiation between fresh and frozen-thawed samples is straightforward, as is differentiation between thawed samples subjected to one or two freeze-thaw cycles. On samples frozen for the second time, it is possible to differentiate between the freezing protocols of the second freezing but not the first freezing. Identification of applied thawing protocols did not appear to be possible with the approach used in this study. Differentiation between freezing protocols is still possible after approximately 12 months of storage. We also find a possible correlation between sample clustering and characteristics relating to perceived quality. These findings could enable the development of technologies for online quality screening of frozen seafood products.

# 6 ACKNOWLEDGEMENTS

We thank the Research Council of Norway for their financial support (194050). The authors also wish to thank Endre Anderssen and Stein Harris Olsen for helpful discussion.

# 7 REFERENCES

Anderssen, E., Dyrstad, K., Westad, F., Martens, H. 2006. Reducing over-optimism in variable selection by cross-model validation Chem. Int. Lab. Sys, 84, 69–74. doi:10.1016/j.chemolab.2006.04.021

Bonilla, A.C., Sveinsdottir, K., Martinsdottir, E., 2007. Development of quality index method (QIM) scheme for fresh cod (Gadus morhua) fillets and application in shelf life study. Food Control 18 (4), 352–358. doi: 10.1016/j.foodcont.2005.10.019

Chen, Y.C. and Pan, B.S. 1997. Morphological changes in tilapia muscle following freezing by air-blast and liquid nitrogen methods. Int. J. Food Sci. Tech. 32, 159–168. doi:10.1046/j.1365-2621.1997.00392.x

Cover, T., Hart, P. 1967. Nearest neighbor pattern classification IEEE Trans. Info. Theo. 13, 21-27 doi: 10.1109/TIT.1967.1053964

Desnosier, N.W., Tressler, D.K. 1977 Fundamentals of Food Freezing. Avi Publishing company.

Duflos, G., Le Fur, B., Mulak, V., Becel, P., Malle, P., 2002. Comparison of methods of differentiating between fresh and frozen-thawed fish or fillets. Journal of the Science of Food and Agriculture 82, 1341–1345. doi: 10.1002/jsfa.1195

ElMasry, G., Wold, J.P., 2008. High-speed assessment of fat and water content distribution in fish fillets using online imaging spectroscopy. J. Agric. Food Chem. 56, 7672–7. doi:10.1021/jf801074s

Hale, G.M., Querry, M.R., 1973. Optical Constants of Water in the 200-nm to 200-microm Wavelength Region. Appl. Opt. 12, 555–63. doi:10.1364/AO.12.000555

Hurling, R., McArthur, H., 1996 Thawing, refreezing and frozen storage effects on muscle functionality and sensory attributes of frozen cod (Gadus morhua). J. Food. Sci., 61, 1289-1296. doi: 10.1111/j.1365-2621.1996.tb10981.x

Jacques, S.L., 2013. Optical properties of biological tissues: a review. Phys. Med. Biol. 58, R37-61. doi:10.1088/0031-9155/58/11/R37

Kent, M., Oehlenschlager, J., Mierke-Klemeyer, S., Knøchel, R., Daschner, F., Schimmer, O., 2004. Estimation of the quality of frozen cod using a new instrument. Eur. Food. Res. Technol. 219, 540-544. doi: 10.1007/s00217-004-0997-z

Love, R.M. 1962 Protein denaturation in frozen fish VI. - Cold storage studies on cod using the cell fragility method

494 J. Sci. Ed, Agric. 13 200. doi: 10.1002/jsfa.2740130501

495 MacCallums, W.A., Laishley, E.J., Dyer, W.J., Idler, D.R. J.P. 1966. Taste panel assment of Cod fillets after single
496 and double freezing. J. Fish. Res. Bd. Canada 23 1063-1081. doi: 10.1139/f66-097

497 Matos, E., Silva, T.S., Tiago, T. Aureliano, M., Dinis, M.T., Dias, J. 2011. Effect of harvesting stress and storage
498 conditions on protein degradation in fillets of farmed gilthead seabream (Sparus aurata): a differential
499 scanning calorimetry study. Food Chem. 126, 270-276. doi: 10.1016/j.foodchem.2010.11.017

500 Mørkøre, T., Lilleholt, R. 2007, Impact of freezing temperature on quality of farmed atlantic cod (Gadus Morhua
501 L.), J. Tect. Stud. 38, 457-472. doi: 10.1111/j.1745-4603.2007.00108.x

502 Nilsen, H., Esaiassen, M., Heia, K., Sigernes, F., 2002. Visible/near-infrared spectroscopy: a new tool for the
503 evaluation of fish freshness? Journal of Food Science 67 (5), 1821–1826. doi: 10.1111/j.1365-
504 2621.2002.tb08729.x

505 Olsen, S.H., Elvevoll, E.O., 2011. pH-induced shift in hemoglobin spectra: a spectrophotometeric comparison of
506 atlantic cod ( Gadus morhua ) and mammalian hemoglobin. J. Agric. Food Chem. 59, 1415–22.
507 doi:10.1021/jf1036273

508 Ottestad, S., Høy, M.,Stevik, A., Wold, J.P. 2009. Prediction of ice fraction and fat content in super-chilled salmon
509 by contact interactance near infrared imaging. J. Near Infrared Spectrosc. 17, 77-87. doi:
510 http://dx.doi.org/10.1255/jnirs.827

511 Pan, B.S. and Yeh, W.T. 1993. Biochemical and morphological changes in grass shrimp (Penaeus monodon)
512 following freezing by air blast and liquid nitrogen methods. J. Food Biochem. 17, 147–160. doi:
513 10.1111/j.1745-4514.1993.tb00464.x

514 Peavy, S., Work, T., Riley, J. 1994 Consumer attitudes towards fresh and frozen fish. J. Aq. Food. Prod. Technol.
515 3, 71-87. http://dx.doi.org/10.1300/J030v03n02_07

516 Pope, R.M., Fry, E.S., 1997. Absorption spectrum (380–700 nm) of pure water II Integrating cavity measurements.
517 Appl. Opt. 36, 8710. doi:10.1364/AO.36.008710

518 Schaare, P.N., Fraser, D.G., 2000. Comparison of reflectance, interactance and transmission modes of visible-
519 near infrared spectroscopy for measuring internal properties of kiwifruit (Actinidia chinensis). Postharvest
520 Biology and Technology 20 (2), 175–184. doi: 10.1016/S0925-5214(00)00130-7

521 Siche, R., Vejarano, R., Aredo, V. , Velasquez, L., Saldanam E., Quevedo, R., 2016. Evaluation of Food Quality and
522 Safety with Hyperspectral Imaging (HSI). Food Eng. Rev. 8: 306-322. doi:10.1007/s12393-015-9137-8

523 Sivertsen, A.H., Chu, C.-K., Wang, L.-C., Godtliebsen, F., Heia, K., Nilsen, H., 2009. Ridge detection with application
524 to automatic fish fillet inspection. J. Food Eng. 90, 317–324. doi:10.1016/j.jfoodeng.2008.06.035

525 Sivertsen, A.H., Kimiya, T., Heia, K., 2011. Automatic freshness assessment of cod (Gadus morhua) fillets by
526 Vis/Nir spectroscopy. J. Food Eng. 103, 317–323. doi:10.1016/j.jfoodeng.2010.10.030

527 Sivertsen, A.H., Heia, K., Hindberg, K., Godtliebsen, F., 2012. Automatic nematode detection in cod fillets (Gadus
528 morhua L.) by hyperspectral imaging. J. Food Eng. 111, 675–681. doi: 10.1016/j.jfoodeng.2012.02.036

529 Sun, D.W. Hyperspectral imaging for food quality analysis and control, 2010, Elsevier

530 Syamaladevi, R.M., Manahiloh, K.N., Muhunthan, B., Sablani, S.S. 2012 Understanding the influence of
531 state/phase transitions on ice recrystallization in Atlantic Salmon (salmo salar) during frozen storage. Food
532 Biophys. 7, 57-71. doi:10.1007/s11483-011-9243-y

533 Tsai, B.K., Allen, D.W., Hanssen, L.M., Wilthan, B., Zeng, J., 2008. A comparison of optical properties between
534 solid PTFE (Teflon) and (low density) sintered PTFE, in: Proc. SPIE 7065, Reflection, Scattering, and
535 Diffraction from Surfaces, 70650Y (August 29, 2008). doi:10.1117/12.798138

536 Tolstorebrov, I., Eikevik, T.M., Bantle, M., 2014. Thermal phase transitions and mechanical characterization of
537 Atlantic cod muscles at low and ultra-low temperatures. J. Food Eng. 128 (0), 111–118.
538 http://dx.doi.org/10.1016/j.jfoodeng.2013.12.025.

539 Velioğlu, H.M., Temiz, H.T., Boyaci, I.H., 2015. Differentiation of fresh and frozen-thawed fish samples using

Raman spectroscopy coupled with chemometric analysis. Food. Chem. 172, 283-290 http://dx.doi.org/10.1016/j.foodchem.2014.09.073

Vidacek, S., Medic, H., Botka-Petrak, K., Nezak, J. Petrak, T. 2008. Bioelectrical impedance analysis of frozen sea bass (Dicentrarchus labrax) J. Food. Eng. 88, 263-271. doi:10.1016/j.jfoodeng.2008.02.010

Warm, K., Bøknæs, N., Nielsen, J. 1998 Development of Quality Index Methods for evaluation of frozen cod (Gadus morhua) and cod fillets J. of Aq. Food Prod. Tech., 7 45–59 doi: 10.1300/J030v07n01_04

Wold, J.P., Johansen, I.R., Haugholt, K.H., Tschudi, J., Thielemann, J., Segtnan, V.H., Narum, B., Wold, E., 2006. Non-contact transflectance near infrared imaging for representative on-line sampling of dried salted coalfish (bacalao). J. of near Infrared Spectroscopy 14 (1), 59–66.

Wold, S., Esbensen, K., Geladi, P. 1987 Principal component analysis Chemometr. Intell. Lab 2, 37-52 doi:10.1016/0169-7439(87)80084-9

Zhu, F., Zhang, D., He, Y., Liu, F., Sun, D.-W., 2013. Application of Visible and Near Infrared Hyperspectral Imaging to Differentiate Between Fresh and Frozen–Thawed Fish Fillets. Food Bioprocess Technol. 6, 2931–2937. doi:10.1007/s11947-012-0825-6